[논 문] 한국재료학회지
Kor. J. Mater. Res.
Vol. 20, No. 4 (2010)

DOI: 10.3740/MRSK.2010.20.4.217

Effect of TaB_2 Addition on the Oxidation Behaviors of ZrB_2-SiC Based Ultra-High Temperature Ceramics

Seung Jun Lee and Do Kyung Kim†

Department of Materials Science and Engineering, Korea Advanced Institute of Science and Technology, 335 Gwahangno, Yusong-gu, Daejeon 305-701, Korea

(Received March 31, 2010 : Received in revised form April 15, 2010 : Accepted April 15, 2010)

Abstract Zirconium diboride (ZrB2) and mixed diboride of (Zr0.7Ta0.3)B2 containing 30 vol.% silicon carbide (SiC) composites were prepared by hot-pressing at 1800°C. XRD analysis identified the high crystalline metal diboride-SiC composites at 1800°C. The TaB2 addition to ZrB2-SiC showed a slight peak shift to a higher angle of 2-theta of ZrB2, which confirmed the presence of a homogeneous solid solution. Elastic modulus, hardness and fracture toughness were slightly increased by addition of TaB2. A volatility diagram was calculated to understand the oxidation behavior. Oxidation behavior was investigated at 1500°C under ambient and low oxygen partial pressure (pO2~10-8 Pa). In an ambient environment, the TaB2 addition to the ZrB2-SiC improved the oxidation resistance over entire range of evaluated temperatures by formation of a less porous oxide layer beneath the surface SiO2. Exposure of metal boride-SiC at low pO2 resulted in active oxidation of SiC due to the high vapor pressure of SiO (g), and, as a result, it produced a porous surface layer. The depth variations of the oxidized layer were measured by SEM. In the ZrB2-SiC composite, the thickness of the reaction layer linearly increased as a function of time and showed active oxidation kinetics. The TaB2 addition to the ZrB2-SiC composite showed improved oxidation resistance with slight deviation from the linearity in depth variation.

Key words ultrahigh-temperature ceramics; composite, hot-pressing, oxidation, mechanical properties.

1. Introduction

In general, transition metal boride, carbide and nitride have been classified as ultra-high temperature ceramics (UHTCs). UHTCs possess unique properties such as high melting point (> 3200°C), mechanical properties, good oxidation resistance and chemical inertness.[1-4] Therefore, interest in UHTCs has increased in the field of aerospace applications such as a thermal protection system (TPS) on hypersonic aerospace vehicles and reusable atmospheric re-entry vehicles. Among UHTCs, ZrB_2 has the lowest theoretical density (6.09 g/cm^3) and has good thermal shock resistance that can be an advantageous for TPS and other aerospace applications.[5,6]

Many attempts have been made to enhance the oxidation resistance of ZrB_2-based materials through appropriate additives. Considerably, the most common additive is SiC which enhance the oxidation-resistance by formation of SiO_2.[1,4] Oxidation behaviors of ZrB_2-SiC composites were well defined by number of investigators.[2,5,7-9] When it is exposed to oxidizing environments (at the temperature of 1500°C), it forms a layer structure: (1) continuous silica rich layer; (2) SiC depletion layer; (3) Un-reacted layer. This surface silica rich layer prohibit the transport of oxygen through the oxide scales and makes ZrB_2-SiC composite possible to show parabolic mass gains kinetics.[2,7] Another approach to improve the oxidation resistance is modification of surface glass layer by addition of second phase such as Ta, TaB_2 and $TaSi_2$.[10-12]

Recently, most of the oxidation tests were conducted in the furnace. Furnace test under an ambient atmosphere, however, is different from the unique environment encountered during re-entry. Furnace test has been carried out in static or flowing air at a fixed temperature under 1 atmosphere. However, during the reentry condition, molecular oxygen will be dissociated due to the impact with at leading wing edge and/or nose cap structure by hypersonic velocity.[13,14] So the O:O_2 ratio, i.e. oxygen partial pressure will be reduced during reentry environment. Thus, along with temperature, oxygen partial pressure also important parameter to evaluate oxidation resistance of UHTCs.

The purpose of this paper is to investigate of the effect of TaB_2 addition into ZrB_2-SiC composite on the oxidation behavior in air and low oxygen partial pressure.

2. Experimental Procedure

2.1 Processing

Commercially ZrB_2 powder (H.C. Starck, Grade A), TaB_2

†Corresponding author
E-Mail : dkkim@kaist.ac.kr (D. K. Kim)

Table 1. Summary of UHTCs compositions, designations, relative density and mechanical properties.

Compositions	Designation	Density (%)[a]	Elastic modulus, E(GPa)	Hardness, H(GPa)	Toughness K_{IC}(MPa $m^{1/2}$)
ZrB_2-30vol%SiC	ZS	99.1	514	19.2 ± 0.7	3.94 ± 0.15
$(Zr_{0.7}Ta_{0.3})B_2$-30val%SiC	ZTS	99.4	546	20.0 ± 0.4	4.35 ± 0.15

[a]Based on rule of mixture

powder (Japan New Metal) and α-SiC powder (H.C. Starck, UF25) were used in this study. To reduce the particle size and increase sintering driving force, as-received ZrB_2 and TaB_2 were vibration milled for 2 h using steel ball and jar. During the milling, 4 wt.% of Fe impurity was introduced because of wear of the steel balls. Fe impurity was removed by an acid treatment. The compositions, designation and processing conditions were summarized in Table 1. The powders were ball-milled in ethanol for 24 h using ZrO_2 milling media. The solvent of the powder mixtures were evaporated on hot-plate with continuous stirring to minimize segregation by sedimentation. Thus, obtained milled powders were hot-pressed (Thermal Technology Inc, Astro Hot Press) in BN-coated graphite dies. The powder compacted was heated under Ar flow at 1800°C with a heating and cooling rate of ~20°C/min. At the saturation point of the die temperature 1800°C, a uniaxial load of 32 MPa was applied and dwelled for 2 h and then cooled to room temperature.

2.2 Characterization

The relative density of the sintered samples was measured using the Archimedes' technique with deionized water as the immersing medium. Phases of hot pressed samples were analyzed by an X-ray diffraction (XRD, Rigaku D/MAM-IIIC). The microstructures of each specimen were observed using a scanning electron microscopy (SEM Philips XL 30). Elastic modulus (E) was measured by the resonance frequency method (ASTM E1876-1, 2001) using an oscilloscope (Tektronix TDS210 w/FFT module) and non-contact transducer (Cirrus ZE:901 CRL L3M Preamplifier). Polished cross-section of the hot-pressed specimens was indented using a Vickers hardness tester (Mitutoyo HM-124) at a contact load of 2 kg for 20 s. And to measure of fracture toughness, the same samples were also Vickers-indented with a higher load of 10 kg for 20 s and radical cracks (2c) were measured in the optical microscope. The fracture toughness was calculated using the following relation[15]: $K_{IC} = 0.016(E/H)^{0.5}Pc^{-1.5}$, where K_{IC} is the fracture toughness, E is elastic modulus, H is hardness, P is load and c is crack length for a center of impression to a crack tip, respectively.

2.3 Oxidation

Oxidation tests were carried out in horizontal tube furnace. Prior to oxidation, all the samples were diamond-polished to a 1 μm using routine metallographic methods. Each specimen was heated a ~10°C/min to the 1500°C and held for 1 h. The oxidation behavior also studied using thermal gravimetric analysis (TGA, SETARAM). The weight change was measured under air at a heating rate of a ~10°C/min up to 1500°C with an isothermal hold for 300 min. In case of low oxidation test, a gas mixture of CO and 2000 ppm of CO_2 was used to produce an oxygen partial pressure of ~10^{-8} Pa at 1500°C. The mixture gas was chosen base on the thermodynamic calculation reported by A. Rezaie.[13] Analogously, heating rate was ~10°C/min to the 1500°C and holding 1 to 10 h in flowing mixture gas.

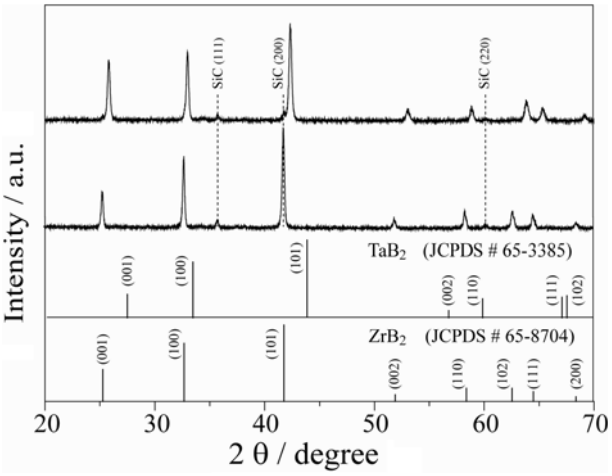

Fig. 1. XRD patterns of materials ZS showing the presence of ZrB_2 and SiC. JCPDS numbers 65-8704 and 65-0360 were used to identify the ZrB_2 and SiC phase, respectively. XRD peaks ZTS were located between ZrB_2 and TaB_2 showing the formation of the solid solution.

3. Results and Discussions

3.1 Microstructure and mechanical properties

The XRD patterns of the hot-pressed samples fabricated at 1800°C for 2 h are shown in Fig. 1. The XRD pattern of ZS shows the presence of ZrB_2 and SiC, no second phases were detected. Based on XRD pattern of ZTS, as the TaB_2 addition in ZS, the slight increase in 2-theta of ZrB_2 was observed. It clarified formation of continuous solid solution between the ZrB_2 and TaB_2.[2,4] Increase in 2-theta indicates that smaller atomic radius Ta (145pm) was

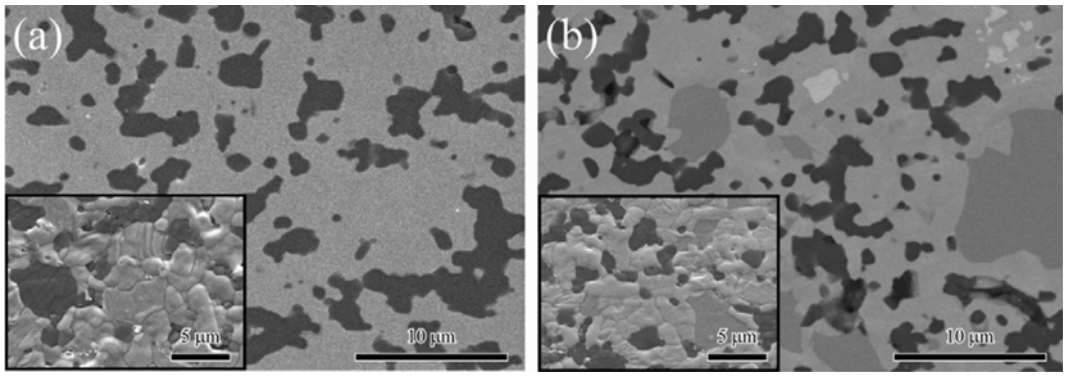

Fig. 2. SEM micrographs of materials: Polished surface of (a) ZS and (b) ZTS. The gray phase is ZrB_2 and the dark phase is SiC. Insets showed the thermal etched image of each material.

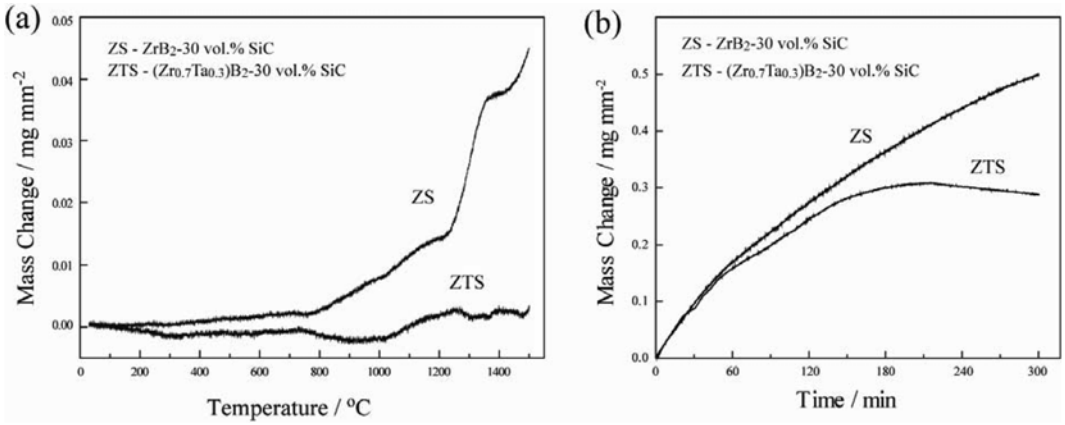

Fig. 3. TGA analysis of the materials in air: (a) changes in the mass as a function of temperature up to 1500°C and (b) isothermal oxidation at 1500°C showing the parabolic oxidation behavior.

substituted with larger atomic radius Zr (155 pm) and decrease in C_0 than original C_0 of ZrB_2 (C_0 : 3.53 Å).

Bulk densities for the hot pressed billets were measured. The results showed 5.17 g/cm^3 of ZS and 6.28 g/cm^3 of ZTS by using a rule of mixture calculation that assumed densities 6.09 g/cm^3 for ZrB_2, 11.7 g/cm^3 for TaB_2 and 3.21 g/cm^3 for SiC, respectively. Based on this true density, all samples had > 99% relative densities. Similar to previous reports, reduced particle size via vibration milling was effective to enhance the driving force in the sintering process.[2,8] Reduced particles had a high surface area that decreases the activation energy for densification. Fig. 2 shows polished surface and inset shows thermal etched surface of ZS and ZTS, respectively. The dark phases, which represent SiC particulate are partly distributed in a clustered formation in the ZrB_2 (gray phase) matrix. In agreement with density measurements, no indication of closed porosity was found in ZS and ZTS. In case of ZS, ZrB_2 grains were equiaxed with a majority of the grains ranging from 1 to 6 μm. In ZTS, grain size of ZrB_2-TaB_2 solid solution was ranging from 0.6 to 4 μm. By addition of TaB_2, the grain size was slightly reduced. Grain shape of solid solution phase grains were similar to ZrB_2 grain shape in ZS. SiC phase also had equiaxed with smaller grain size (0.8 to 1.6 μm) than boride phase.

Mechanical properties of hot pressed composites are summarized in Table 1. Room temperature elastic modulus (E) of ZS is 514 GPa which is slightly higher than reported value.[2,4] And elastic modulus of ZTS is 546 GPa. The increase in the elastic modulus may due to the addition of stiffer material such as TaB_2 (686 GPa). It was clear that addition of high elastic modulus leading to a better elastic modulus in ZS composition. Similarly, the hardness and fracture toughness also slightly increased by addition of TaB_2.

3.2 Oxidation Behavior

Fig. 3(a) shows the changes in the mass as a function of temperature in air. And the results of isothermal (300 min) TGA analysis at 1500°C are shown in Fig. 3(b). All samples show a negligible mass gain below 800°C. In ZS, the mass gain starts at 800°C and continuous mass gain was observed to 1200°C. The mass gain might be related to oxidation of ZrB_2 (*s*) to B_2O_3 (*s*) and ZrO_2 (*s*) by reaction (1).[6,13] And above the 800°C, the mass change related to the mass loss due to the vaporization of the

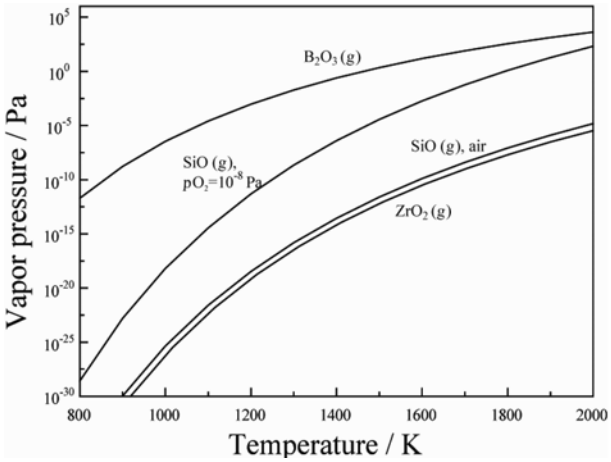

Fig. 4. Volatility diagram of some oxide calculated at ambient and low oxygen partial pressure ($pO_2 = 10^{-8}$ Pa). Volatility diagrams of SiO (*g*) is largely depend on oxygen partial pressure. Oxygen is neither consumed nor produced in ZrO_2, B_2O_3, the vapor pressure of ZrO_2 (*g*), B_2O_3 (*g*) does not vary with pO_2.

B_2O_3 and mass increase due to the formation of ZrO_2. Mass gain was a slowdown around 1200°C, this might due to the significant vaporization of B_2O_3 by reaction (2). The vaporization of B_2O_3 is explained by the volatility diagram (Fig. 4). The vaporization range for B_2O_3 (*l*) in air is expected to be low at 800°C based on the partial pressure of the various gases. However, at the temperature of 1200°C, the predominant vapor species in air was B_2O_3 (*g*) with a pressure of ~10^{-3}. Two other species have vapor pressure predicted to be lower than 15 orders of magnitude. And based on the 8 order of a magnitude increase in the pressure of the dominant species in compared to 800°C, the rate of B_2O_3 (*l*) vaporization would be expected to be significantly higher at 1200°C, which is consistent with B_2O_3 evaporation from the surface of ZrB_2 and remains ZrO_2 (*s*).[7]

$$ZrB_2\ (s) + 5/2O_2\ (g) \rightarrow ZrO_2\ (s) + B_2O_3\ (l) \quad (1)$$

$$B_2O_3\ (l) \rightarrow B_2O_3\ (g) \quad (2)$$

Active oxidation of ZrB_2 and SiC is occurred at the region that there is no surface Si rich glass. Therefore, sharp increase of weight gain in ZS after 1200°C may be attributed to the localized surface Si rich layer. Similarly, mass gain starts at 1000°C in ZTS which is higher temperature than ZS, and this mass gain might be related to the oxidation of ZrB_2 and TaB_2 to ZrO_2 and Ta_2O_5, respectively. Similar to previous work,[10,11] mixed boride influences on a small increase of the weight gain up to 1500°C and this improvement in oxidation resistance is attributed to the phase separation.[11] In case of ZS, as mentioned above, sharp increase of mass was observed after 1200°C, but during the isothermal analysis at 1500°C in Fig. 3(b), shape of the curves with a decrease of the rate of the oxidation versus time, i.e. parabolic oxidation was observed.[2,7] This phenomenon is related to the formation of surface SiO_2 rich layer.[3,7,13] The increase of surface coverage by Si rich glass with a time is related to the parabolic oxidation kinetic in ZS. As shown in the Fig. 3(b), ZTS shows higher oxidation resistance and this may be attributed to formation of corresponding oxide (Ta_2O_5) in the surface Si rich glass. It is known from the literature that borate and silicate glasses containing Group IV-VI transition metal oxides show a strong tendency to phase separation.[10,11] Systems showing immiscibility are characterized by sharply rising liquidus temperatures and increased viscosity. Increased viscosity of surface Si rich glass reduces oxygen diffusion through the surface glass and weight gain is decreased.

Fig. 5 shows cross-sectional SEM images of the oxidized materials at 1500°C for 60 min in air. Oxidation of ZrB_2-SiC composites at 1500°C produced structures that consist of three layers: (I) surface silica-rich layer, (II) SiC-depleted layer, and (II) un-reacted layer. The formation of three layers is consistent with the previous reports.[2,7-9,13,15] At high temperature (above 1300°C), SiC phase begins oxidizing, resulting in the formation of a silica-rich glassy

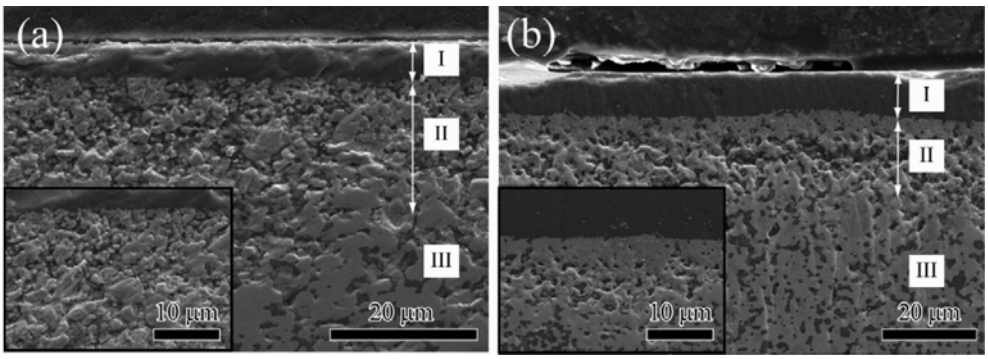

Fig. 5. Cross-sectional SEM micrographs of oxidized materials (1500°C, 60 min, in air). (a) ZS and (b) ZTS showing a layered structure: uniform layer of SiO_2 (I), SiC depleted layer (II) and un-reacted ZrB_2-SiC layer (III). The oxidized layer of ZTS beneath the SiO_2 layer appears less porous than the observed in the ZS.

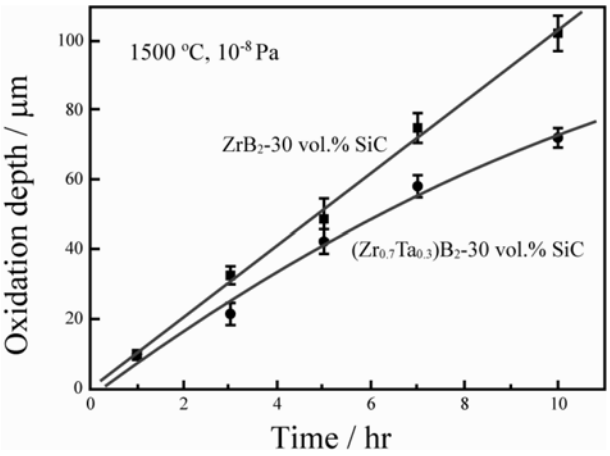

Fig. 6. Variations of the reaction layer thickness with time for exposures of the samples to CO- 2000 ppm CO_2 mixture gas at 1500°C. The linear trend suggests reaction rate-controlled kinetics.

layer by reaction (3).

$$SiC\ (s) + 3/2O_2\ (g) \rightarrow SiO_2\ (l) + CO\ (g) \quad (3)$$

The SiO_2 layer remains protective up to at least 1700°C as SiO_2 is significantly less volatile than B_2O_3 (by Fig. 4). The surface SiO_2 layer acts as a barrier for inward oxygen transport.[2,7,13] Thus, a silica-rich layer that provides the passive oxidation behavior with parabolic kinetic to ZS and ZTS as shown in Fig. 3(b). SiC depletion layer, inset of Fig. 5(a), which was located underneath the surface Si rich layer, had a porous structure due to the active oxidation of SiC. The microstructure of this region was similar to the original structure before oxidation, except that the SiC was removed by active oxidation according to reaction (3). However, in ZTS (inset of Fig. 5(b)), the oxidized layer beneath the surface SiO_2 layer appears less porous than that observed in the ZS. This may be the result of the Ta_2O_5-SiO_2 liquid phase having a higher viscosity because of phase separation, leaving it less vulnerable to capillary extraction to the amorphous surface layer.[10,11] The less porous oxide layer would then likely be more protective of the underlying diboride than the analogous layer in the ZS Therefore, the layer impedes the oxygen diffusion to the inner scale. Along an increase in the viscosity of surface SiO_2 layer with a formation of less porous oxide layer, oxygen diffusion was decreased and the amount of oxidation of inner scale was decreased. Therefore, ZTS showed a less mass gain and improved oxidation resistance as shown in the isothermal TG analysis (Fig. 3(b)).

Fig. 6 shows the variations of the thickness of the oxidized layer as a function of oxidation time in an oxygen partial pressure of 10^{-8} Pa at 1500°C. As shown in Fig. 6, the thickness of reaction layer appeared to increase linearly with time in ZS. The linear trend suggests a reaction rate-controlled kinetics. According to the volatility diagram in Fig. (4), the vapor pressure of SiO (*g*) is high

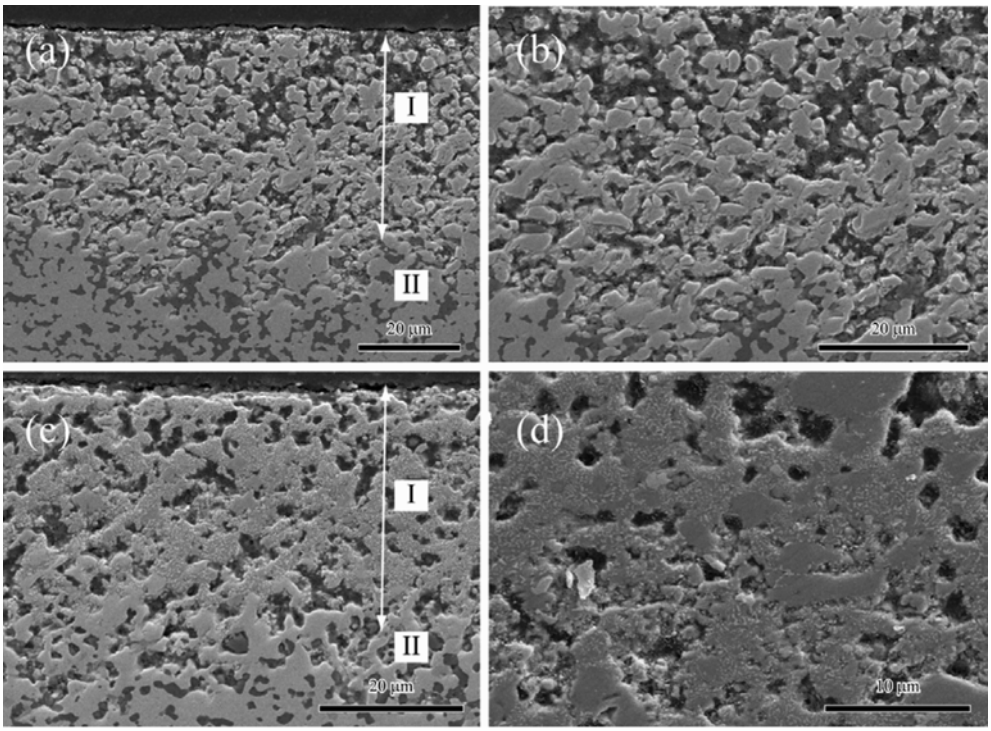

Fig. 7. SEM micrographs of (a), (b) ZN and (c), (d) ZTS after oxidation in oxygen partial pressure of 10^{-8} Pa. ZT and ZTS showing a layered structure: oxidized layer (I) and un-reacted ZrB_2-SiC layer (II). The oxidized layer of ZTS appears less porous than the observed in the ZS.

in this oxygen partial pressure. Because of the high vapor pressure of SiO (*g*), the SiC was removed by active oxidation according to reaction (4) and surface protective layer could not be formed.

$$SiO_2\ (l) \rightarrow SiO\ (g) + 1/2O_2\ (g) \quad (4)$$

Fig. 7 shows SEM cross-sectional images of ZN and ZTS after oxidation test for 60 min under oxygen partial pressure of ~10^{-8} Pa at 1500°C. Similar to the previous report,[12,16] there exist two layers, i.e. SiC depletion layer and un-reacted layer. So the porous SiC depletion layer in ZS cannot act as a protective layer for oxygen diffusion unlike the surface SiO_2 layer observed in Fig. (5). SiC-depletion layer consisted of porous ZrO_2 allows direct transport of oxygen to the reaction interface and reaction rate-controlled kinetics will be predicted. In Fig. 6, the reaction layer of ZS increased 9.8 ± 1.3 to 102.4 ± 5.1 μm when the exposure time increased from 1 to 10 h. In case of ZTS, the reaction layers were increased from 10.1 ± 1.2 to 72.3 ± 2.8 μm with time increase from 1 to 10 h. According to the reaction layer analysis, ZTS shows higher oxidation resistance and slightly deviated from the linearity in depth variation (Fig. 6). This may also due to the formation of less porous oxide layer. And the formation of less porous oxide layer might be related to particle rearrangement and/or densification by means of low melting point of Ta_2O_5 (1872°C).

4. Conclusions

Fully densified ZrB_2 and $(Zr_{0.7}Ta_{0.3})B_2$ contained 30 vol.% SiC composite materials were prepared by a hot-pressing at the temperature of 1800°C. XRD analysis identified the high pure crystalline metal diboride-SiC composites at 1800°C. The TaB_2 addition to ZrB_2 -SiC samples showed a slight peaks shift to higher angle of 2-theta of ZrB_2 that confirmed homogeneous solid solution. Mechanical properties were slightly increased by addition of TaB_2.

In an ambient oxidation test, ZrB_2-SiC and $(Zr_{0.7}Ta_{0.3})B_2$-SiC showed parabolic oxidation behavior at 1500°C. TaB_2 addition to ZrB_2-SiC showed the improved oxidation resistance attributed to phase separation in surface Si rich glass with increased viscosity and formation of less porous oxide layer beneath the surface SiO_2. Oxidation test at low oxygen partial pressure of ~10^{-8} Pa at 1500°C produced a double layer structure due to the high vaporization of SiO (*g*). In ZrB_2-SiC composite, thickness of reaction layer linearly increased as a function of time. However, TaB_2 addition to ZrB_2-SiC showed improved oxidation resistance with slightly deviated from the linearity by formation of less porous oxide layer. TaB_2 addition to ZrB_2-SiC improved oxidation resistance in air and low oxygen partial pressure.

Acknowledgment

This work was financially supported by Brain Korea 21 (BK21) program and by Priority Research Centers Program through the National Research Foundation of Korea (NRF) funded by the Ministry of Education, Science and Technology (2009-0094041). S.J.L. would like to thank the Fundamental R&D Program for Core Technology of Materials funded by the Ministry of Commerce, Industry and Energy.

Reference

1. Y. B. Lee, J. S. Kim, S. B. Kim, H. C. Park and K. D. Oh, Kor. J. Mater. Res., **9**(1), 8 (1999) (in Korean).
2. W. G. Fahrenholtz and G. E. Hilmas, J. Am. Ceram. Soc., **90**(5), 1347 (2007).
3. S. J. Lee and D. K. Kim, Sur. Rev. Lett., **17**(3), 1 (2010).
4. N. P Bansal, Handbook of ceramics composite, p.197, Springer, US (1997).
5. J. Han, P. Hu, X. Zhang and S. Meng, Scripta. Mater., **57**, 825 (2007).
6. W. W. Wu, G. J. Zhang, Y. M. Kan and P. L. Wang, J. Am. Ceram. Soc., **91**(8), 2501 (2008).
7. A. Rezaie, W. G. Fahrenholtz and G. E. Hilmas, J. Eur. Ceram. Soc., **27**, 2495 (2007).
8. S. J. Lee and D. K. Kim, Key Eng. Mater., **403**, 253 (2009).
9. S. N. Karlsdottir and J. W. Halloran, J. Am. Ceram. Soc., **91**(1), 272 (2008).
10. E. Opila, S. Levine and J. Lorincz, J. Mater. Sci., **39**, 5969 (2004).
11. M. M. Opeka, I. G. Talmy and J. A. Zaykoski, J. Mater. Sci., **39**, 5887 (2004).
12. D. Sciti, L. Silvestroni, G. Celotti and S. Guicciardi, J. Am. Ceram. Soc., **91**(10), 3285 (2008).
13. A. Rezaie, W. G. Fahrenholtz and G. E. Hilmas, J. Am. Ceram. Soc., **89**(10), 3240 (2006).
14. A. Bongiorno, C. J. Först, R. K. Kalia, J. Li, J. Marschall, A. Nakano, M. M. Opeka, I. G. Talmy, P. Vashishta and S. Yip, Mater. Res. Soc. Bull., **31**, 410 (2006).
15. S. S. Hwang, A. L. Vasiliev and N. P. Padture, Mater. Sci. Eng. A, **464**, 216 (2007).
16. M. Balat, G. Flamant, G. Male and G. Pichelin, J. Mater. Sci. **27**, 697 (1992).